

Analysis of the DebrisSat Fragments and Comparison to the NASA Standard Satellite Breakup Model

James Murray¹, Heather Cowardin¹, J.-C. Liou², Marlon Sorge³, Norman Fitz-Coy⁴, and Tom Huynh⁵

⁽¹⁾Jacobs, NASA Johnson Space Center, 2101 NASA Parkway, Mail Code XI5-9E, 2101 NASA Parkway, Houston, TX 77058, USA, james.i.murray@nasa.gov

⁽²⁾NASA Orbital Debris Program Office, NASA Johnson Space Center, Mail Code XI5-9E, 2101 NASA Parkway, Houston, TX 77058, USA

⁽³⁾The Aerospace Corporation, 2155 Louisiana Blvd. NE #5000, Albuquerque, NM 87110, USA

⁽⁴⁾University of Florida, nfc@ufl.edu

⁽⁵⁾Air Force Space and Missile Systems Center, 483 North Aviation Blvd, El Segundo, CA 90245, USA

ABSTRACT

Existing DOD and NASA satellite breakup models are based on a key laboratory test, the 1992 Satellite Orbital debris Characterization Impact Test, which has supported many applications and matched on-orbit events involving older satellite designs reasonably well over the years. In 2014, the NASA Orbital Debris Program Office, in collaboration with the Air Force Space and Missile Systems Center, The Aerospace Corporation, and the University of Florida, conducted a hypervelocity impact test using a high-fidelity, mock-up satellite, DebrisSat, in controlled and instrumented laboratory conditions to update and improve these models. DebrisSat is representative of present-day, low Earth orbit satellites, having been constructed with modern spacecraft materials and techniques. The DebrisSat fragment ensemble provided a variety of shapes, bulk densities, and dimensions. Fragments down to 2 mm in size are being characterized by their physical and derived properties. The data will inform updates to the current NASA Standard Satellite Breakup Model (SSBM), which was formulated using laboratory and ground-based measurements of on-orbit fragmentation events to describe an average breakup for spacecraft and upper-stage collisions and explosions. Although individual fragment collection and characterization is still ongoing, this paper will present the status of the DebrisSat fragment data analysis including cumulative characteristic length and cumulative mass distributions, area-to-mass distributions, and characteristic length versus mass distributions. Additionally, comparisons to the NASA SSBM will be presented.

1 INTRODUCTION

The DebrisSat project is a collaboration of the NASA Orbital Debris Program Office (ODPO), the Air Force Space and Missile Systems Center (SMC), The Aerospace Corporation (Aerospace), and the University of Florida (UF). The project has four primary goals: 1) design and fabricate a 56-kg class spacecraft (“DebrisSat”) representative of modern spacecraft in the low Earth orbit (LEO) environment; 2) conduct a hypervelocity laboratory impact test to simulate a catastrophic fragmentation event of DebrisSat; 3) collect, measure, and characterize all fragments down to 2 mm in size; and 4) use the data to improve space situational awareness applications and satellite breakup models for better orbital debris environment definition [1].

Existing DOD and NASA satellite breakup models are based on a key laboratory test, Satellite Orbital debris Characterization Impact Test (SOCIT), which was conducted by the Department of Defense (DOD) and NASA at the Air Force Arnold Engineering Development Complex (AEDC) in 1992 to support the development of satellite breakup models. The main target for SOCIT was a fully functional U.S. Navy Transit 1960’s era satellite. The DOD and NASA breakup models based on the SOCIT data have supported many applications and matched on-orbit events reasonably well over the years [1].

As new materials and construction techniques are developed for modern satellites; however, there is a need for new laboratory-based tests to acquire data to improve the existing DOD and NASA breakup models. The need for such tests also is supported by discrepancies between model predictions and observations of fragments generated from the breakup of modern satellites, including the Iridium 33 and Fengyun 1-C [2]. The DebrisSat project is an outgrowth of this need.

The DebrisSat design was based on a survey of modern satellites in LEO [3, 4]. All major design decisions, including the selection of components, subsystems, mass fractions, structure, and construction methods were reviewed and approved by subject matter experts from Aerospace. In addition, the DebrisSat body was covered with multi-layer insulation (MLI) and three solar panels were attached to one side of the main body (Fig. 1).

To reduce the project cost, a decision was made to emulate the majority of components. The emulated components were based on existing designs of flight hardware, including structure, dimensions, materials, avionics components, and connection mechanisms. At the end of assembly, DebrisSat was subjected to a NASA General Environmental Verification Specification qualification vibration test to ensure the integrity of the fabrication/assembly process.

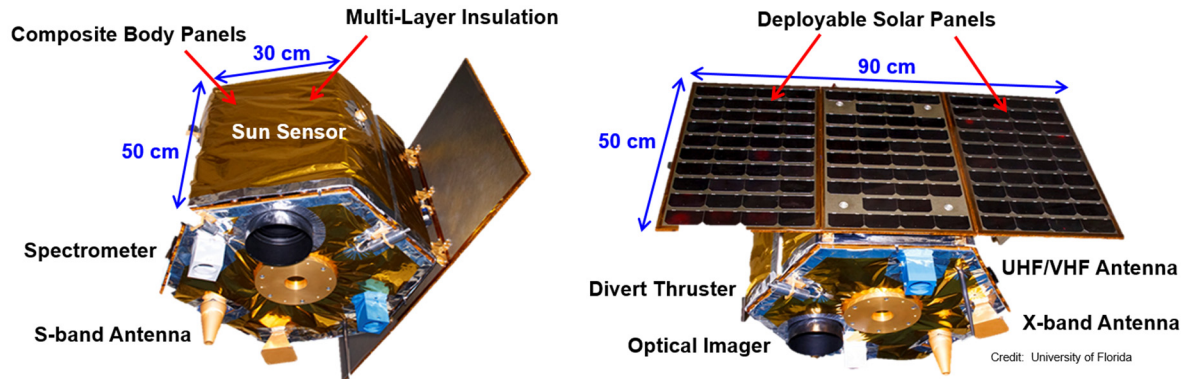


Fig. 1. DebrisSat design.

To increase the project's benefits further, Aerospace designed and built a target resembling a launch vehicle upper stage ("DebrisLV") for the pre-test shot; details of the two targets are listed in Table 1. The pre-test shot was conducted two weeks prior to the DebrisSat impact test with identical conditions to DebrisSat (facility set-up, projectile, and impact speed). The resulting fragments, carefully collected and stored in boxes, will be characterized after DebrisSat characterization is complete.

Another key element implemented in DebrisSat and DebrisLV hypervelocity impact tests was the use of a soft catch system inside the chamber. In the SOCIT test series the foam catch system, which consisted of panels, was used only in the downrange and sideways directions. Based on lessons learned from the SOCIT impact test, the DebrisSat project increased the thickness of the soft-catch foam panels and fully covered the interior of the target chamber with these panels to prevent any fragments from impacting the chamber walls, which would produce secondary damage not associated with the breakup. Table 1 also compares some SOCIT, DebrisSat, and DebrisLV test conditions.

2 DEBRISAT BACKGROUND

From 2009-2014 the planning and fabrication for the DebrisSat and DebrisLV were in process. On 1 April and 15 April 2014, respectively, the DebrisLV and DebrisSat impacts were successfully carried out at AEDC Range G. To maximize the projectile mass at the 7 km/sec impact speed without a sabot, the AEDC team developed a special projectile design featuring a hollow aluminum cylinder embedded in a nylon cap. The nylon cap served as a bore rider for the aluminum cylinder to prevent hydrogen leakage and to protect the two-stage light gas gun barrel [1].

Table 1. SOCIT, DebrisSat, & DebrisLV Test Comparison

	SOCIT/Transit	DebrisSat	DebrisLV
Target body dimensions	46 cm (dia) × 30 cm (ht)	60 cm (dia) × 50 cm (ht)	35 cm (dia) × 88 cm (ht)
Target mass	34.5 kg	56 kg	17.1 kg
MLI and solar panel	No	Yes	No
Projectile material	Al sphere	Hollow Al cylinder with attached nylon bore-rider	Hollow Al cylinder with attached nylon bore-rider
Projectile dimension/mass	4.7 cm diameter, 150 g	8.6 cm × 9 cm, 570 g	8.6 cm × 9 cm, 598 g
Impact speed	6.1 km/sec	6.8 km/sec	6.9 km/sec

	SOCIT/Transit	DebrisSat	DebrisLV
Impact Energy to Target Mass ratio (EMR)	81 J/g (2.8 MJ total)	235 J/g (13.2 MJ total)	832 J/g (14.2 MJ total)
Soft-Catch System: Polyurethane foam stacks	3 densities: 0.06, 0.096, and 0.192 g/cm ³ ; 25 cm thick	3 densities: 0.048, 0.096, and 0.192 g/cm ³ ; up to 61 cm thick	3 densities: 0.048, 0.096, and 0.192 g/cm ³ ; up to 51 cm thick

After the impacts of DebrisLV and DebrisSat, all intact foam panels, broken foam pieces, loose fragments, and dust were carefully collected, processed, documented, and placed in bags or plastic containers for shipping to a storage facility. The initial estimates using the NASA Standard Satellite Breakup Model (SSBM) indicated the number of 2 mm (and larger) fragments from DebrisSat and DebrisLV were approximately 85,000 and 35,000, respectively. Since August 2014, the UF team has been working to extract fragments from foam panels, characterize each fragment down to 2 mm in size, and upload the data into a database.

3 FRAGMENT CHARACTERIZATION

The project's primary goal is to recover at least 90% of the total DebrisSat mass from the fragments and to measure the physical properties of all recovered fragments. To achieve this goal, all fragments with at least one dimension ≥ 2 mm are carefully collected and/or extracted from the foam panels/pieces and assigned unique identification numbers before their physical characteristics are determined. A priority of the characterization process is to develop and implement methodologies to minimize biases and/or errors associated with "human-in-the-loop" activities during measurements.

During the characterization process, each fragment's physical (observed and derived) parameters are archived in the DebrisSat Categorization System (DCS). The DCS is a database solution designed and developed specifically to manage the large amounts of data generated by the DebrisSat project. The list of parameters is shown in Table 2. In addition to the information shown in Table 2, associated metadata (e.g., location the fragment was found within the chamber, images of the fragments, etc.) are also archived in the DCS.

The characterization process is broken into three major categories: Assessment, Measurement, and Calculation. In this process, the initial step involves assessing each uniquely identified fragment in terms of material, shape, color, and what imaging system the fragment qualifies for: two dimensional (2D) or three dimensional (3D) imaging. To expedite the large number of fragments, duplicate 2D imagers and one 3D imager are available. Smaller, flat fragments are measured in the 2D imaging systems, while larger objects up to $55 \times 55 \times 55$ mm in volume are processed using the 3D system. For larger objects, an alternative scanning system will be utilized. Details on the imaging systems can be found in [5]. After assessments are completed, the measurement process acquires the mass and physical size based on the solid body (SB) dimensions (X_{SB} , Y_{SB} , and Z_{SB}). The last step in the characterization process involves calculating the characteristic length (L_c), the average of the object's three maximum orthogonal projected dimensions (X_{DIM} , Y_{DIM} , and Z_{DIM}); average cross-sectional area; and volume. Details on how the volume dimensions are calculated can be found in [6]. The process undergoes thorough verification checks to ensure repeatability and reproducibility on a recurring basis.

Table 2. Fragment parameters captured in database.

Parameter	Definition/Notes
Unique ID with associated barcode	Earlier studies grouped multiple, similar small fragments to get average characteristics
Material	Predefined categories based on as-built design; material density is auto-populated once material is selected.
Shape	Flat Plate Bent Plate Straight Needle/Rod/Cylinder Bent Needle/Rod/Cylinder Parallelepiped/Nugget/Spheroid Flexible/MLI
Color	Predefined categories based on as-built design
Principle dimensions	x, y, z (mm) {relative to solid body coordinates}
Characteristic length	$L_c = (X_{DIM} + Y_{DIM} + Z_{DIM})/3$ (mm)
Average cross-sectional area	Weighted average of projected areas visible in multiple 2-D images; pixel-to-length (and area) relationship calculated from hardware characteristics and scene geometry (mm ²).

Parameter	Definition/Notes
Mass	Fragment mass (g)
Area-to-mass ratio (AMR)	Calculated average cross-sectional area divided by measured mass (mm ² /g).
Volume	Calculated from point cloud using convex hull and alpha-shape subtraction (mm ³).
Bulk Density	Measured mass divided by calculated volume (g/mm ³).

Figure 2 and Fig. 3 provide an update of the status of the data collection process. Based on the mass of the target, projectile, and impact velocity, the expected number of fragments generated using the NASA SSBM was estimated to be close to 85,000, shown in Fig. 2. After one year of collection, the number of collected fragments surpassed the amount projected by the SSBM and is increasing as the project continues.

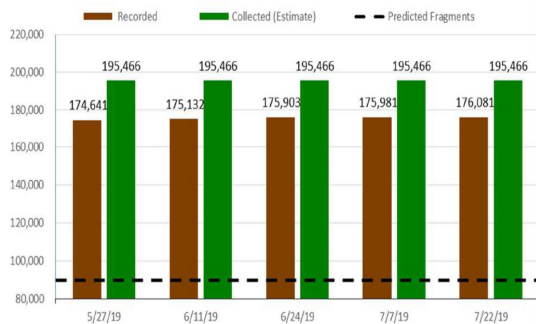


Fig. 2. Historical progression of recorded/collected fragments.

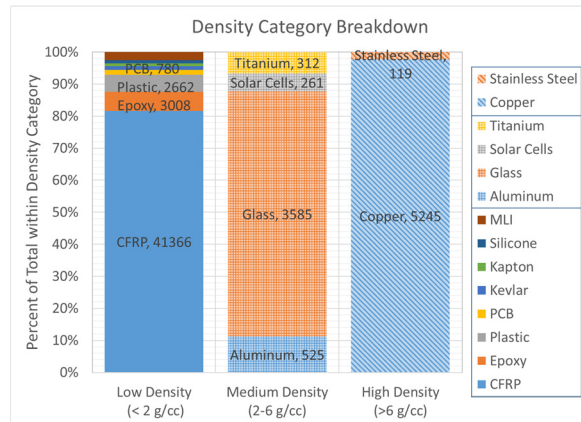


Fig. 3. Fragment breakdown by material/density type. Current as of 22 July 2019.

4 SHAPE CATEGORIZATION

As summarized in Table 2, six shape categories have been defined that allow DebrisSat fragment shapes to be uniquely described. A rubric developed by the project team allowed workers to categorize unambiguously what may otherwise have been a process prone to subjective assessment when measuring the X_{SB} , Y_{SB} , and Z_{SB} dimensional triplets; this rubric is illustrated in Fig. 4; Fig. 5 reflects the actual rubric. The solid body (SB) of a fragment is the box that best represents the shape of the object and contains at least 75% of the SB. SB dimensions are used in qualitative shape assessment and are distinct from the x, y, and z dimensions calculated for L_c .

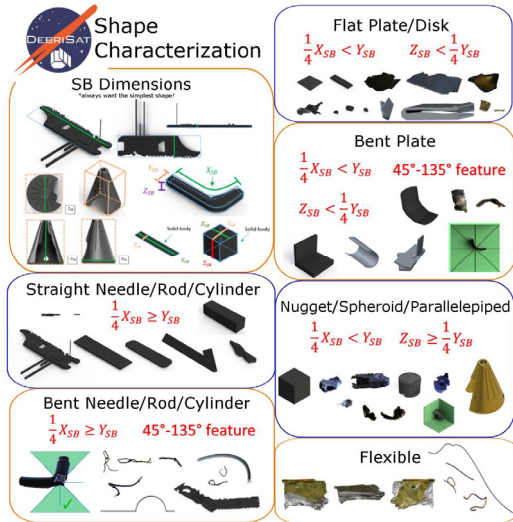


Fig. 4. Fragment shape categorization rubric.

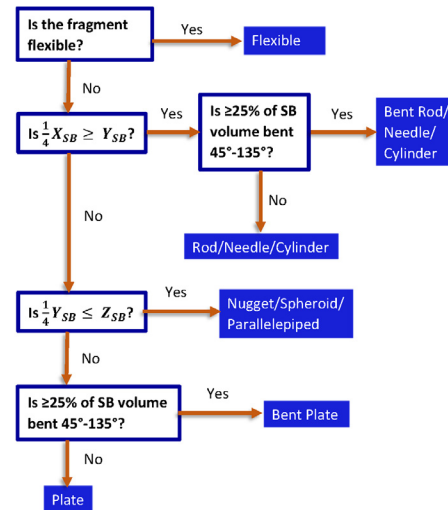


Fig. 5. Illustrated shape categories in general order of rubric "Yes."

5 NASA STANDARD SATELLITE BREAKUP MODEL

The NASA SSBM was formulated using laboratory tests and ground-based remote measurements of on-orbit fragmentation events to provide an average breakup ensemble for spacecraft and upper stage collisions and explosions. Following significant validation efforts against observable data, including the development of a radar Size Estimation Model (SEM) based on SOCIT fragments [7], the SSBM was deployed in EVOLVE 4.0, NASA’s long-term, Monte Carlo, environment simulation, computer program [8]. The SSBM is described in detail in [9], which also describes other U.S. Government debris models.

The SSBM uses L_c as the fundamental independent variable in lieu of mass. This choice of L_c in preference to mass was driven by the on-orbit observables, namely Two Line Element (TLE) orbital data sets and radar cross section (RCS) time series. The TLE sets provide sufficient information to determine or infer number of fragments and their post-event orbits, the area-to-mass ratio (AMR), and separation velocities for members of specific breakup event ensembles. The RCS time series provide sufficient information to infer L_c and area. Orbital data was used to derive and validate distributions for $L_c > 11$ cm. Laboratory data, including the SOCIT [10] and the ESA Ariane subscale model explosion series, were essential in defining the distributions below approximately 8 cm, and a bridging function was applied to the 8-11 cm L_c gap. Distributions in cumulative number, area, and AMR for collision and explosion fragments are provided by the SSBM; the cumulative number distribution for collisions additionally incorporates mass characteristics of the event to model catastrophic and non-catastrophic collisions. The separation velocity (Δv) distribution uses AMR as its independent variable.

The NASA Engineering Safety Center (NESC) provided guidance for the Orbital Debris Engineering Model (ORDEM) update that resulted in the deployment of ORDEM 3.0, specifically including mass density as a parameter, which was accomplished in ORDEM 3.0. To accommodate this new parameter, the SSBM ensemble functions were partitioned by mass density. This was done by integrating SOCIT density data into three major density categories [11] for fragments between 1 mm and 10 cm in L_c (objects larger than 10 cm are assigned the nominal density of 2.8 g/cm³). The density categories are shown in Table 3.

Table 3. SSBM Density Bins.

Low Density	< 2.0 g/cm ³	Nominal Low Density	1.4 g/cm ³
Medium Density	2.0 – 6.0 g/cm ³	Nominal Medium Density	2.8 g/cm ³
High Density	> 6.0 g/cm ³	Nominal High Density	7.9 g/cm ³

The AMR is monitored to ensure that a given statistical sampling from the distribution does not result in an object denser than is reasonable in a given category—the consequence of which would be unrealistically long orbital lifetimes. Based on the ORDEM 3.0 and NASA BUMPER II impact risk models, the high- and medium-density categories pose the principal risk to resident space objects. The NASA Debris Assessment Software (DAS) v. 2.1.1 [12] also incorporates ORDEM 3.0 and the effects of mass density on probabilistic risk assessment for compliance with NASA Technical Standard 8719.14A, the Process for Limiting Orbital Debris.

The NESC also recommended that shape be included in the breakup ensemble, which will be included in the ORDEM 4.0 development. Analysis of the DebrisSat and DebrisLV datasets will allow for the current three-category density distribution to be further refined into an effective density distribution and, for the first time, shape effects. Incorporation of debris fragment shape into ORDEM 4.0 requires characterization of observed space object signatures as observed by ground-based assets. To apply shape characteristics to remote data used for ORDEM 4.0, a subset of DebrisSat fragments will be further analyzed in laboratory radar and optical facilities to update the existing radar-based NASA SEM and develop a comparable optical-based SEM. Planned activities focused on assessing fragment characterization via laboratory tests (optical and radar) are discussed in [9].

6 CURRENT RESULTS

6.1 Characteristic Length versus Mass

The current SSBM uses L_c as the primary parameter in the cumulative number distribution. During implementation of the breakup model, total mass of the parent body must be conserved, which necessitates ascribing a mass to the debris object drawn from the cumulative number distribution based on L_c [13]. Figure 6 shows the L_c to mass distribution of the largest 100 SOCIT fragments and the least squares fit to the distribution that serves as the relationship between L_c and mass for the SSBM. Additionally, the DebrisSat fragments are also shown, broken out into the SSBM low, medium, and high density categories. The medium density fragments appear to have the same slope as the SOCIT fit, which is consistent since the majority of SOCIT fragments were aluminum (medium density). Within the high density group, there appear three separate clusters. The stainless steel comprises the top-most cluster. The remaining two clusters are both composed of copper, the only other high-density material. The reason for the split is currently unknown, but the split does not seem related to shape category, as both clusters of copper are comprised of varied shapes.

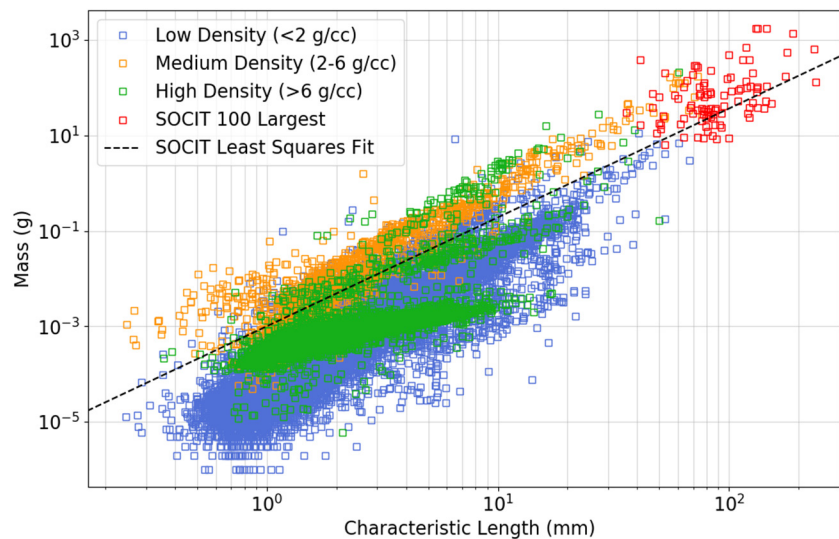


Fig. 6. Characteristic length versus mass distribution broken into SSBM density categories. The dashed line represents the least squares fit to the SOCIT characteristic length versus mass distribution. Current as of 22 July 2019.

A final interesting feature is that when moving to lower sizes, the data, particularly low density debris, begins to deviate in slope from the SOCIT fit line. The slope begins to deviate at just under 1 cm and has a distinctly different

slope by 1 mm. This may provide insight into the SSBM's current tendency to underestimate the number of debris objects produced at 1 mm and overestimate the number produced at 1 cm, when compared to radar data.

6.2 Cumulative Distributions in Characteristic Length and Mass

Much of the current fragment distribution analysis has focused on the cumulative number distributions as a function of L_c . Figure 7 shows the cumulative number distribution of fragments as a function of L_c broken down into the DebrisSat material categories. Each point on the curves represents the total number of fragments of size L_c or larger. The SSBM cumulative number distribution for impacts is expressed as

$$N(L_c) = 0.1M^{0.75}L_c^{-1.71}$$

where L_c is the characteristic length and M is the total mass of the object. Figure 7 also overlays the predicted number of fragments where the total mass M is replaced with the collected mass to date.

So far, the majority of fully characterized fragments have been carbon-fiber reinforced polymer (CFRP); 27,354 of the 40,021 fully characterized fragments, or approximately 68%, are CFRP. This is due to an initial focus on the characterization of the CFRP fragment over the other material categories, a sampling effect that explains the current predominance of CFRP in the cumulative number distributions. Overall, the cumulative number distribution matches well with the current model.

Figure 8 shows the cumulative number distribution of fragments as a function of mass broken down into the DebrisSat material categories. The SSBM prediction for the cumulative number distribution for DebrisSat is shown, scaled to the total mass collected to date, where the SOCIT fit was used to perform L_c -to-mass conversion. The cumulative distribution differs significantly in slope from the model, which can be attributed to the deviation of the DebrisSat data from the SOCIT L_c -to-mass conversion.

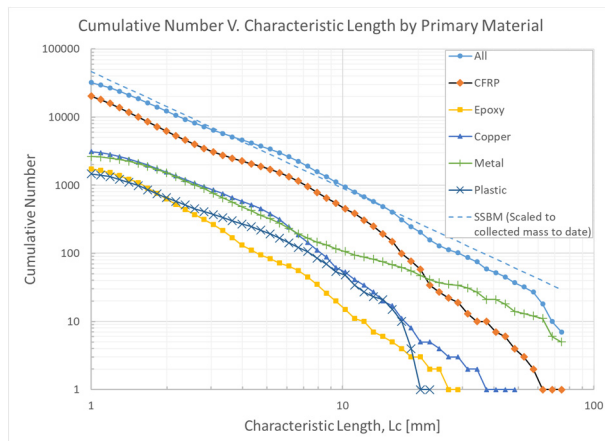


Fig. 7. Cumulative number of fragments versus characteristic length, broken out by material. Current as of 22 July 2019.

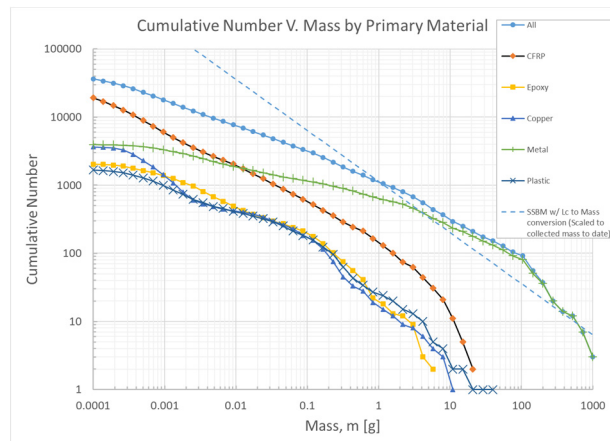


Fig. 8. Cumulative number of fragments versus mass, broken out by material. Current as of 22 July 2019.

6.3 Area-to-Mass Ratio versus Characteristic Length

In general, the SSBM models the L_c to AMR distribution using a bi-Gaussian in $\log_{10} L_c$ - $\log_{10} AMR$ space, where the means and variances are functions of $\lambda_c = \log_{10} L_c$. In the three-density SSBM, the means and variances are different for each density category. For collisions, like DebrisSat, the distribution simplifies to a single Gaussian. Figure 9 shows the L_c to AMR distribution of low-density DebrisSat fragments broken out into the DebrisSat shape categories. The dashed lines represent the mean as provided by the SSBM. The dotted lines represent the standard deviation as provided by the SSBM. In most cases, the SSBM mean appears to be low when compared to the data. The greatest agreement appears in the “nugget” shape category.

Figure 10 shows the L_c to AMR distribution of medium-density DebrisSat fragments broken out into the DebrisSat shape categories. The medium density fragments appear to match the model better, which is consistent with the agreement of medium density fragments with the SOCIT L_c -to-mass model. There appears to be a deviation from

the main cluster of points below 1 mm. The cause is currently unknown but the effect could be seen in multiple shape categories.

Figure 11 shows the L_c to AMR distribution of high-density DebrisSat fragments broken out into the DebrisSat shape categories. Like the low density fragments, the model mean appears to be lower than the data for most shape categories and overall. However, like all other categories, the “nuggets” appear to fit the SSBM mean best.

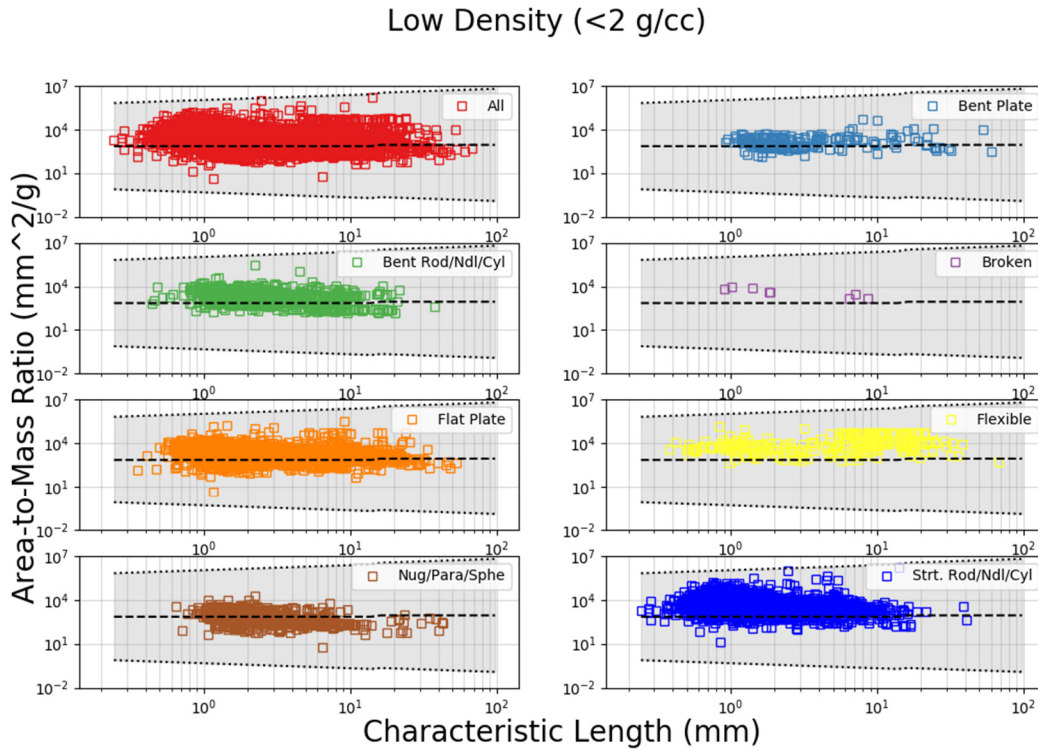


Fig. 9. L_c to AMR distribution for low-density fragments broken out into the DebrisSat shape categories. Current as of 22 July 2019.

Medium Density (2-6 g/cc)

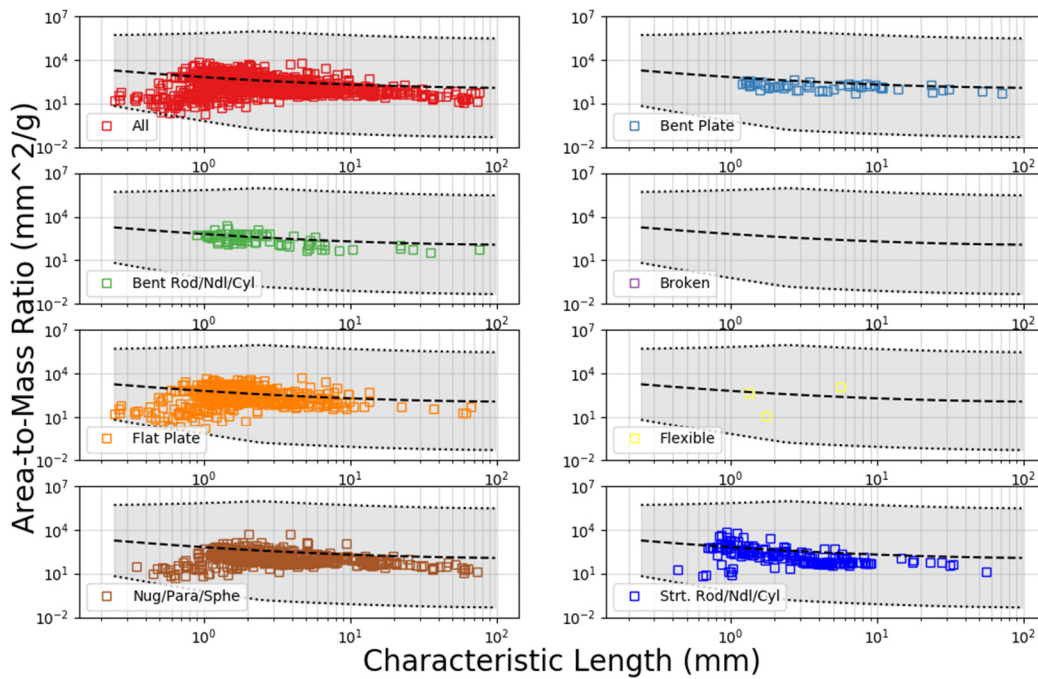


Fig. 10. L_c to AMR distribution for medium density fragments broken out into the DebrisSat shape categories. Current as of 22 July 2019.

High Density (>6 g/cc)

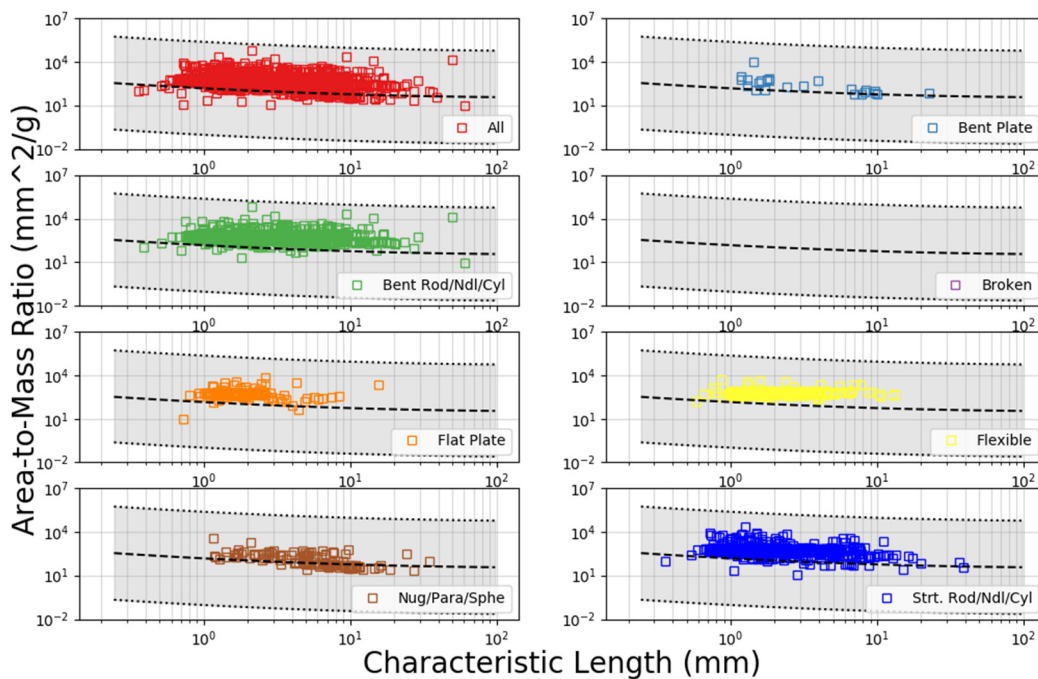


Fig. 11. L_c to AMR distribution for high density fragments broken out into the DebrisSat shape categories. Current as of 22 July 2019.

7 SUMMARY

This paper reviewed the DebrisSat project's motivation; the data collection plan and its status; fragment characterization and categorization by shape; and current modeling and risk assessment activities. Currently, the DebrisSat ensemble is dominated by CFRP (mass density), and nuggets and plates (shape); this may segue to other densities and shapes as the data collection incorporates larger fragments and discrete components.

The DebrisSat data was compared to the SSBM cumulative number distribution and was shown to agree. Additionally, comparisons to the L-to-mass model were made showing agreement for larger fragments and medium density fragments, but deviations for high and low density fragments, especially below 1 mm. Finally, comparisons to the three density SSBM L_c-to-AMR distributions were made in which medium density fragments showed the greatest agreement with the model, particularly "nugget" shaped fragments.

Ongoing fundamental measurement and analytical work will be incorporated into next-generation models for space object characterization, the orbital debris environment model, and risk assessment.

8 REFERENCES

1. Liou, J.-C., *et al.* "Successful Hypervelocity Impacts of DebrisLV and DebrisSat," Orbital Debris Quarterly News vol. 18, issue 3, pp. 3-6, 2014.
2. Liou, J.-C. "An Update on Recent Major Breakup Fragments," Orbital Debris Quarterly News vol. 13, issue 3, pp. 5-6, 2009.
3. Werremeyer, M. Design of Sub-systems for a Representative Modern LEO Satellite, Dissertation, University of Florida, 2013.
4. Clark, S. Design of a Representative LEO Satellite and Hypervelocity Impact Test to Improve the NASA Standard Breakup Model, Dissertation, University of Florida, 2013.
5. Shiotani, B. "Characterizing DebrisSat Fragments: So Many Fragments, So Much Data, and So Little Time," 68th International Astronautical Congress, Adelaide, Australia, 25-29 Sep. 2017.
6. Moraguez, M. *et al.* "An imaging System for Automated Characteristic Length Measurement of DebrisSat Fragments," 66th International Astronautical Congress, Jerusalem, Israel, 12-16 Oct. 2015.
7. Xu, Y., *et al.* "A Statistical Size Estimation Model for Haystack and HAX Radar Detections," IAC 2005.
8. Johnson, N.L., *et al.* "NASA's New Breakup Model of EVOLVE 4.0," Adv. Space Res. 28(9), pp. 1377-84, 2001.
9. Cowardin, H., *et al.* "Characterization of Orbital Debris via Hyper-velocity Laboratory-Based Tests," Proc., 7th European Conf. Space Debris, ESA, 2017.
10. Krisko, P.H., Horstman, M., Fudge, M.L. "SOCIT4 collisional-breakup test data analysis: with shape and material characterization," Adv. Space Res. 41(7), pp. 1138-46, 2008.
11. Krisko, P.H., *et al.* "Material Density Distribution of Small Debris in Earth Orbit," IAC-08.A6.2.1, 2008.
12. Opiela, J., Vavrin, A. "New Version of DAS Now Available," Orbital Debris Quarterly News vol. 21, issue 1, pp. 4-7, 2017.
13. Krisko, P. "Proper Implementation of the 1998 NASA Breakup Model," Orbital Debris Quarterly News vol. 15, issue 4, pp. 4-5, 2011.